

Growth and Inhibition of Equatorial Anomaly Prior to an Earthquake (EQ): Case Studies with Total Electron Content (TEC) Data for Major EQs of Japan 2011 and Indonesia 2012

Minakshi Devi*, Alaka Medhi, Arup Jyoti Dev Sarma, Ananda Kumar Barbara

Department of Physics, Gauhati University, Guwahati, India.

Email: *md555@sify.com

Received April 13th, 2013; revised May 12th, 2013; accepted May 27th, 2013

Copyright © 2013 M. Devi *et al.* This is an open access article distributed under the Creative Commons Attribution License, which permits unrestricted use, distribution, and reproduction in any medium, provided the original work is properly cited.

ABSTRACT

The processes leading to the growth and inhibition of equatorial anomaly before major earthquake (EQ) were viewed in this paper by examining global Total Electron Content (TEC) that contoured over longitude sectors covering Africa to Pacific, in association with EQ events of Japan ($M = 9$) that occurred at 135°E to 145°E and 35°N to 40°N , on March 9 and 11, 2011 and of Indonesia ($M = 8.6$) that took place at 2.311°N , 93°E , in April 11, 2012. The paper focuses on the development of abnormal increase in density in the night sector around -10° latitude zone prior to the two major EQ events, though their epicenters are separated widely from the anomaly region. The F-layer density variations from relevant locations and TEC features obtained from GPS at Appleton anomaly crest station are utilized as supporting inputs. The possible sources leading to the anomalous development in density are discussed in the frame of EQ time consequences of lithospheric-atmospheric processes between the equator and beyond. The role of electric field generated by pre EQ preparatory activities and dynamical coupling modes through seismic fault line are brought in to the ambit of discussion.

Keywords: TEC Global; Earthquake; Equatorial Anomaly; F-Layer Density

1. Introduction

Ionospheric parameters as tools for prediction of an earthquake have been adapted by many workers [1-7]. However, solar geomagnetic influences on ionosphere being significant, the processes of filtering the earthquake (EQ) induced effects from these parameters are difficult exercises. The situation becomes more complex at Appleton anomaly zone [8-11] where ionisation density is transported up by equatorial electric field (E) through EXB drift process. Therefore, at off equatorial stations *i.e.*, round Appleton Anomaly region ($\pm 20^{\circ}$ geomagnetic latitudes), the ionisation density and Total Electron Contents (TEC), have a strong component of migrating electron density. Such movement is also possible from epicentre region during EQ time electric field generated in its preparatory processes [12-14]. Added to these aspects, the anomaly zone undergoes changes with

solar geomagnetic environments as well as on coupling dynamics between equatorial and magnetospheric processes [15-18], thereby making EQ time density changes on TEC or ionisation density around the anomaly as multifactor events [19-21]. There are also reports showing apparent modifications in ionisation density and on TEC by pre earthquake influences on lower atmosphere [22-26].

All these activities make identification of earthquake related dynamics over extended latitudinal and longitudinal sectors very complex especially when anomaly feature is adapted as a tool of EQ precursor as the paper aims. Here, we analyze the growth and inhibition pattern of anomaly zone from global TEC data covering sectors from east Africa to west pacific; the feature so obtained is examined in association with major Japan EQ (JEQ) of March 11, 2011 epicentre at 38.322°N , 142.369°E ($M = 8.9$) and Indonesia EQ (IEQ, $M = 8.6$) of April 11, 2012 occurred at 2.311°N , 93°E . The two events are so se-

*Corresponding author.

lected that EQ time anomaly coupling dynamics could be brought in to focus at widely separated zones around and beyond equatorial anomaly region limited within $\pm 20^\circ$ geomagnetic latitudes. TEC data collected from the GPS receiving setup at Guwahati ($26^\circ 10'N$, $91^\circ 45'E$) along with F-layer peak density (NmF2) data from relevant stations are used as supporting inputs.

2. Observations

A representative profile of TEC obtained from dual frequency GPS observation at Guwahati, an anomaly crest station ($26^\circ 10'N$, $91^\circ 45'E$) is presented in **Figure 1**, to highlight a few features that will be utilized in the analysis to follow. The figure shows that the diurnal TEC reaches its maximum not at the local noon as expected (point A in the figure) but one or two hours from it (marked as B in the figure). Such enhancements in density after the local noon hours are generally associated with the sources at the equator from where electron density is pushed up by the EXB drift process, to be moved down along the field lines to off equatorial region, enhancing the total density at the recipient location. This is the Appleton anomaly phenomenon, described in brief in the introduction. The position of the peak density depends on magnitude of E field and also on the time of its appearance, although in general, the phenomenon is significant in post noon hours as shown in **Figure 1**. In this paper we would examine growth and inhibition of such anomaly zones from global TEC data over wide longitude sectors, the features so obtained will be associated with the two major EQs as described.

2.1. Abnormal Appearance of Anomaly Zone Prior to Japan EQ (JEQ)

The very strong JEQ of March 11, 2011, was preceded by another event of March 9 with $M = 7.3$ occurring at

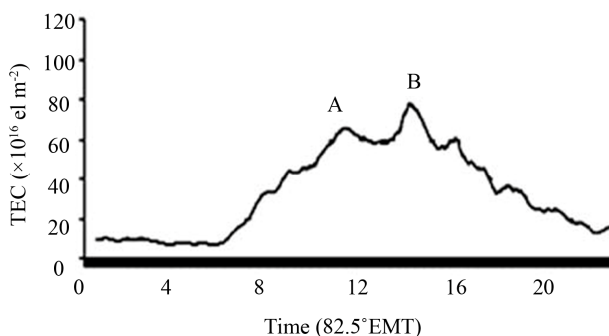


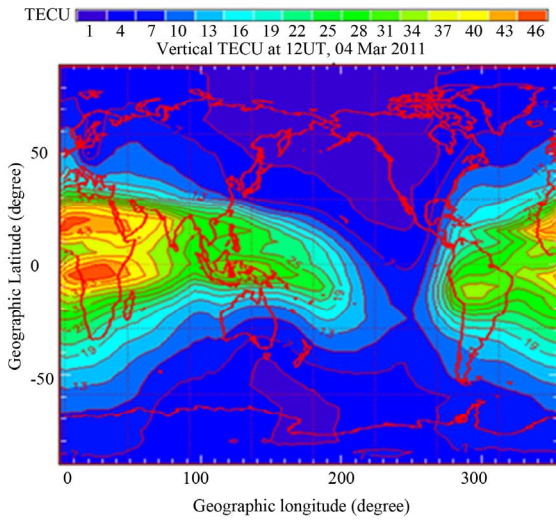
Figure 1. TEC diurnal variation, a representative profile of Guwahati, an equatorial anomaly crests station. Note that the day time TEC maximum occurs at around 1400 hrs (marked as B), instead of at the local noon hours (marked as A).

$38.322^\circ N$, $142.369^\circ E$; the global TEC maps prior to, during and after these events obtained from the Australian meteorological department (www.ips/satellite.au) are presented in **Figures 2(a)-(d)**. The TEC contour plots of the figures correspond to 11 UT - 12 UT, *i.e.* when epicentre zone of $130^\circ E$ to $140^\circ E$ falls in the night sector, so that abnormality if any could be easily identified from relatively low background night time density. **Figure 2(a)** shows TEC situation seven days prior to the EQ when a fully developed equatorial anomaly was present, as expected, at the $20^\circ E$ longitude at 12UT *i.e.* around local noon near East African zone. This is the Normal Equatorial Anomaly (NEA) at $20^\circ E$ off equatorial region. But 6 days prior to the JEQ, the NEA at $20^\circ E$ longitude during local daytime had dissipated but a high dense TEC region is formed in the eastern sector in the longitude range $100^\circ E - 140^\circ E$ at 12UT, *i.e.*, at the local midnight (**Figure 2(b)**) hours. This abnormal appearance of high density zone *i.e.*, “EQ time Equatorial Abnormality” (EEA) is seen up to March 8. On March 9 *i.e.* the day of one of the strongest EQs, the anomaly shifts to NEA sector of $20^\circ E$ to reappear again as EEA at $100^\circ E - 140^\circ E$ longitude on March 10 before the devastating EQ of March 11. The EEA gradually weakens and disappeared after the EQ as shown in **Figure 2(d)**. However, the unusual development of such anomaly though weak, lasted for the entire month associated with the number of relatively small EQs, as an aftereffect of the JEQ.

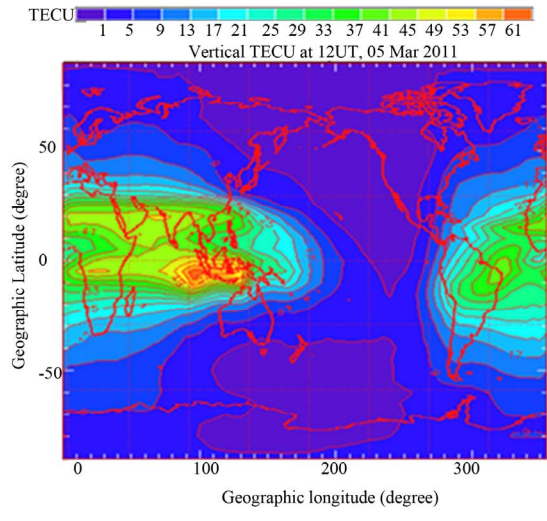
2.2. Abnormal Appearance of Anomaly Zone Prior to Indonesia EQ (IEQ)

The IEQ, that occurred at the epicentre $2.3^\circ N$ and $93^\circ E$ on April 12, 2012 is one of the strongest in recent times with magnitude of $M = 8.6$. We present in **Figure 3** the global TEC map before, during and after this event. More than 6 days prior to the IEQ **Figure 3(a)**, the NEA, as expected, was seen in the African sector ($20^\circ E$) at local day hours (11 UT-13 UT). But 4 days before the event, the NEA of $20^\circ E$ zone dissipates and an EEA appears synchronously in the western Pacific sector showing large accumulation in TEC at around $-10^\circ N$ and $90^\circ E - 100^\circ E$ longitude, *i.e.* during the local midnight (**Figure 3(b)**). The TEC map further shows presence of a fully developed EEA to the day of the EQ and its disappearance following the IEQ (**Figure 3(c)**). The significant point to be noted is that, while the EEA was formed around $100^\circ E - 140^\circ E$ longitude prior to the JEQ, before the IEQ the EEA was seen at $90^\circ E - 100^\circ E$, that is near to the longitude sectors of the epicentre of each event. We also note a few more cases of abnormal high density zones during night sector and around the EEA zone, the reference of which is brought in the sections to follow.

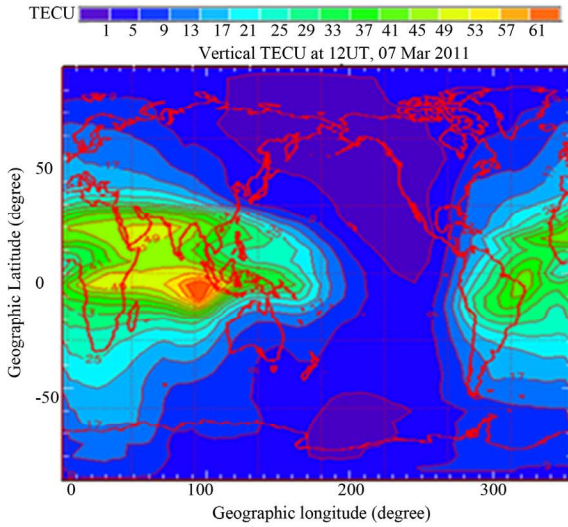
Growth and Inhibition of Equatorial Anomaly Prior to an Earthquake (EQ): Case Studies with Total Electron Content (TEC) Data for Major EQs of Japan 2011 and Indonesia 2012



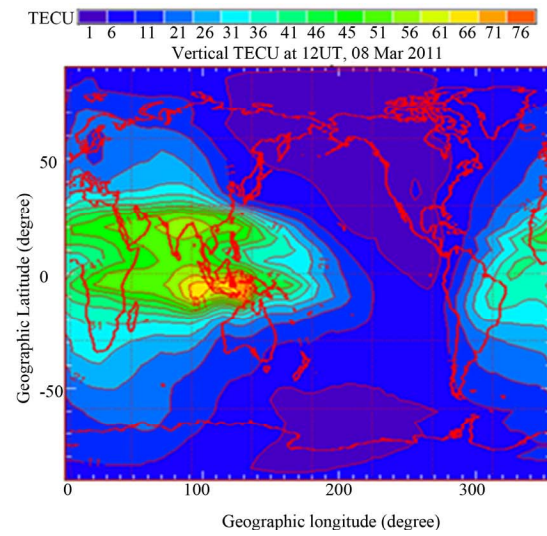
(a)



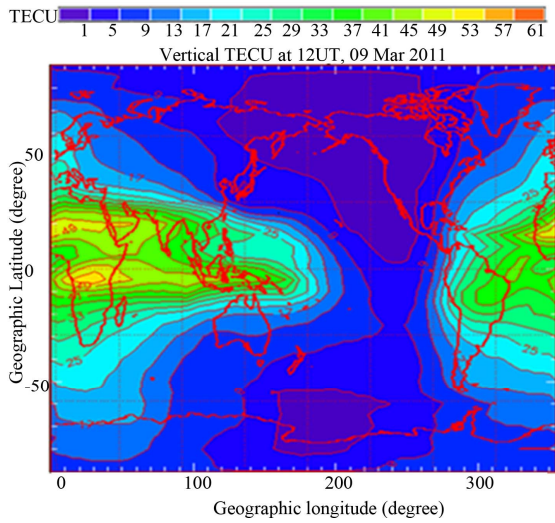
(b)



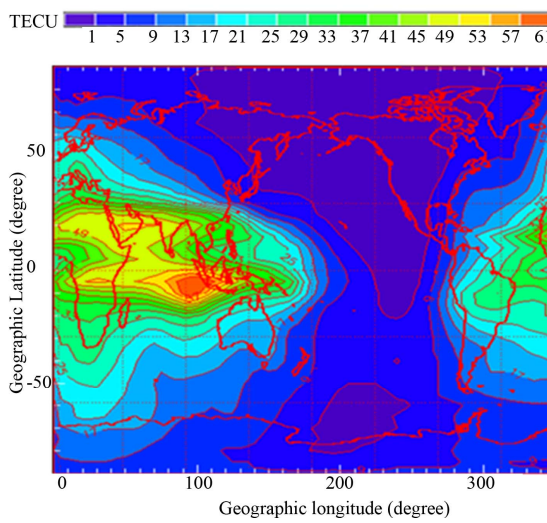
(c)



(d)



(e)



(f)

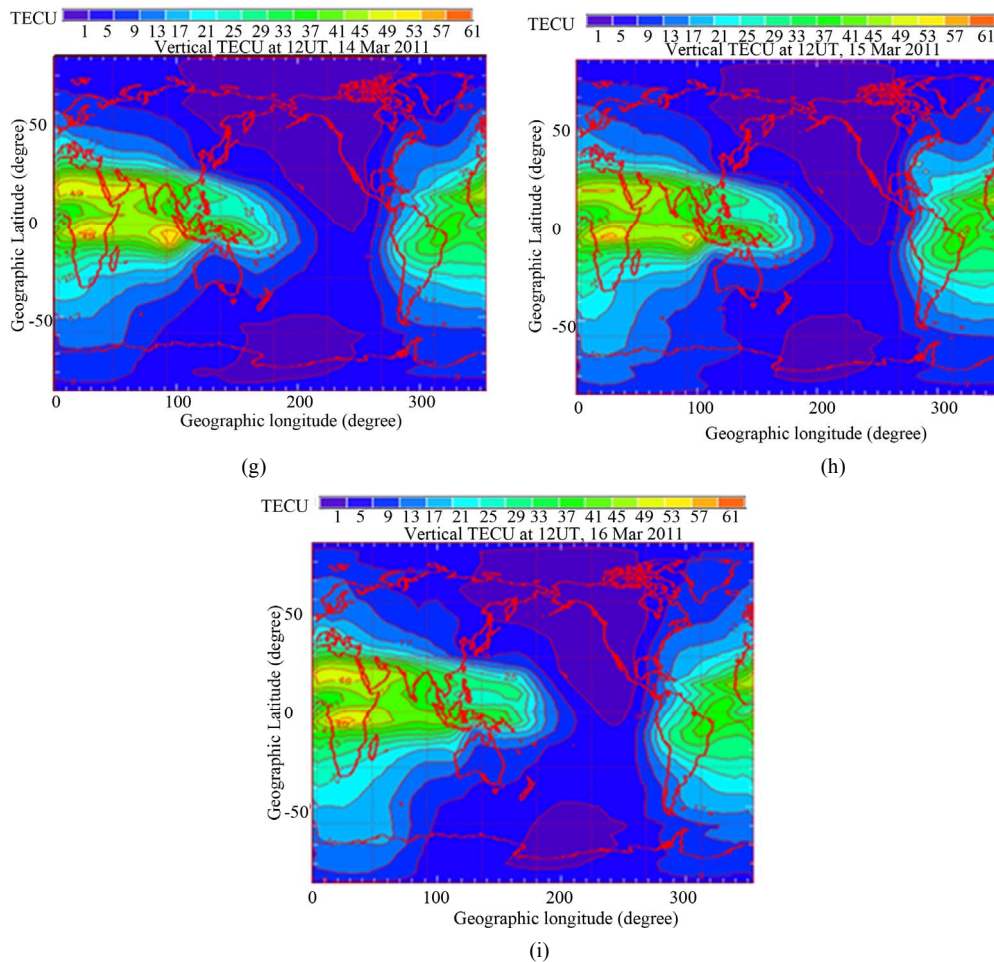


Figure 2. TEC global map displaying (a) development of Normal Equatorial Anomaly (NEA) at 11 UT - 12 UT in 20°E (*i.e.*, around local noon hours), 6 days prior to EQ; (b)-(d) growth of Earthquake time Equatorial Anomaly (EEA) at the night sector in 110°E - 140°E as Japan EQ (JEQ) of March 9, 2011 approaches; (e) disappearance of the EEA and growth of NEA on the day of the EQ; (f) re-development of the EEA prior to the massive EQ of March 11 and (g-i) gradual decay of EEA strength and recovery of NEA after the EQs .

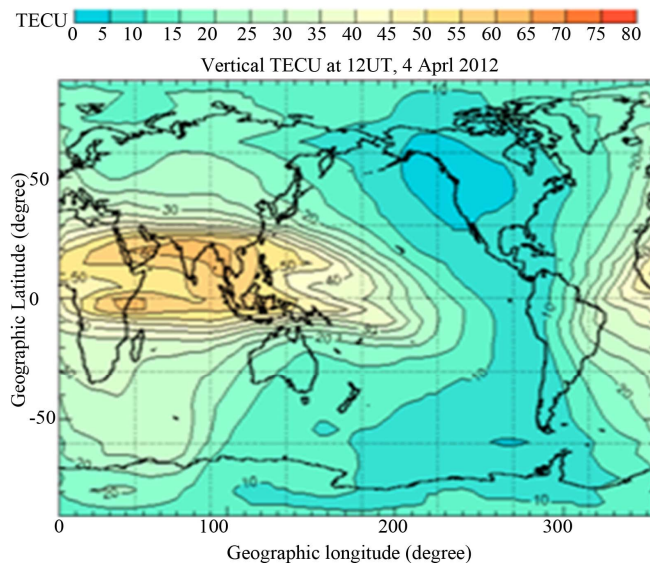
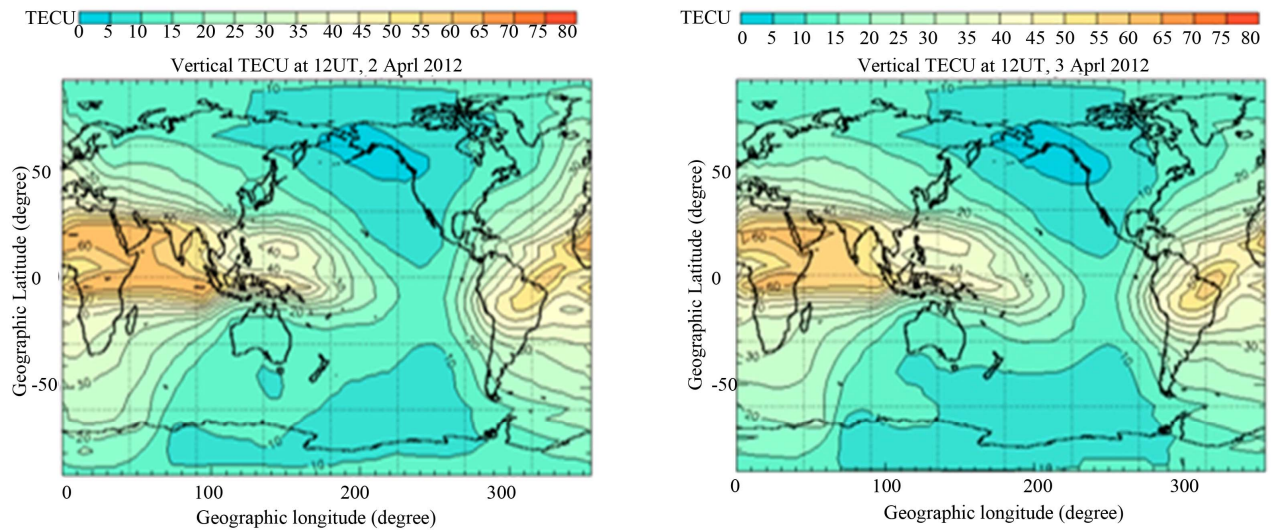
2.3. Association between Magnitude of EEA and Earthquakes in the Longitude Sector 90°E to 145°E

The magnitude of EEA is determined from the increase in TEC value within the anomaly zone with respect to ones prevailing in the NEA zone at that hour and also the longitudinal spread of the EEA. Adopting these two aspects, the EEA strength is defined in grades (arbitrary unit) from 0.5 to 10, with 40 TEC U as minimum value of the TEC and 80 TECU as the maximum, during the period 10 UT -12 UT. The magnitude so derived is presented from March 1 to 15, 2011 in **Figure 4(a)**, also shown in **Figure 4(b)** the strength of EQ events occurring within -10°N to 45°N ; 90°E to 145°E covering the latitudinal /longitudinal zones of the two selected EQs.

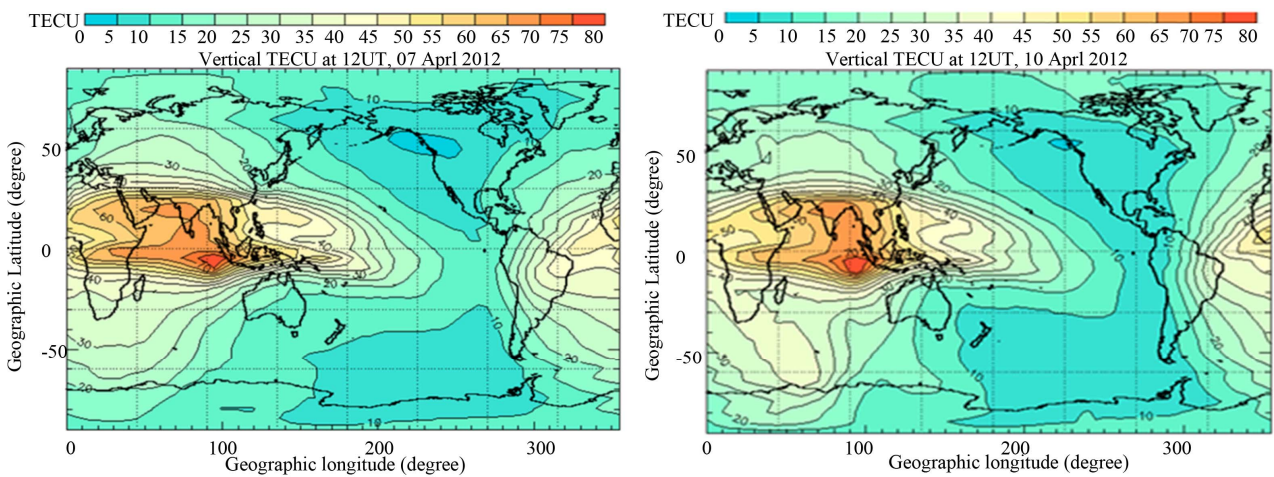
The figures show that the magnitude of EEA increased prior to both the JEQs of March 9 and 11 with a sharp

decrease on the day of the event. However, this result does not isolate the effects on the EEA of large number of relatively small EQs (**Figure 4(b)**) occurring on the same day within this large latitude-longitude area. To identify the EEA with JEQ we now take the earthquake events that occur only within the narrow longitude and latitude zone of 120°E - 140°E and 30°N - 40°N (around the epicentre of JEQ) as shown in **Figure 5(a)**. One can note from **Figure 4(b)** and **Figure 5** that magnitude of EEA increased just before the JEQ events and reverts back to low value on the day of the earthquake, suggesting presence of a strong link between growth of EEA and the JEQs.

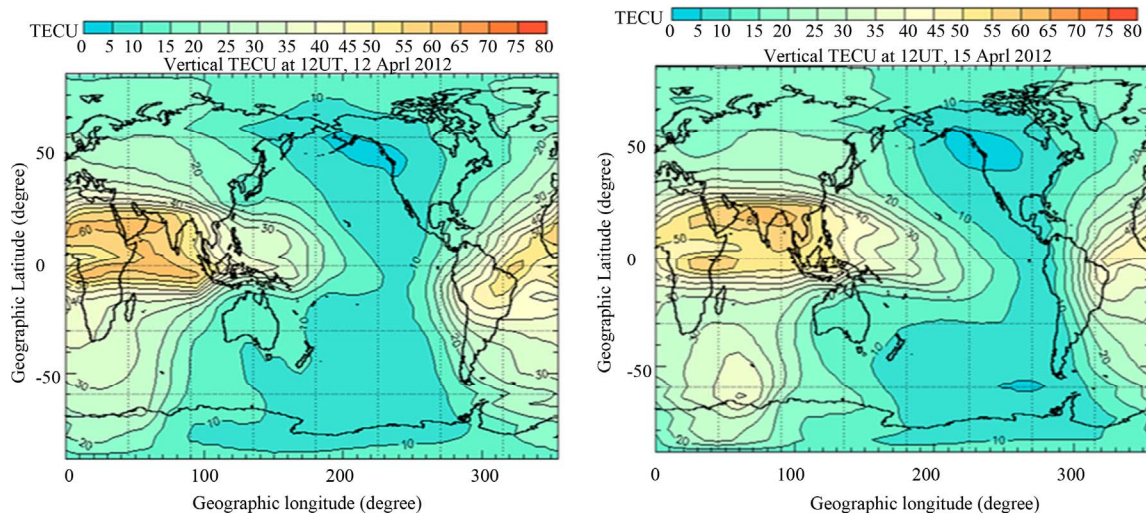
This observation receives support as we do not see any systematic relation between the EEA magnitude (**Figure 4(b)**) and the equatorial EQ events as shown in **Figure 6**, also that no strong equatorial EQ event occurred during this period and within the longitude zone where EEA was



(a)



(b)



(c)

Figure 3. TEC global map displaying (a) development of NEA at 11UT-12 UT around 20°E zone (*i.e.* around local noon hours), about a week prior to Indonesia EQ (IEQ) of 12 April 2012; (b) growth of EEA in 100°E zone during the night sector and disappearance of NEA as the EQ day approaches and (c) disappearance of EEA and the growth of NEA on the day of the event and after.

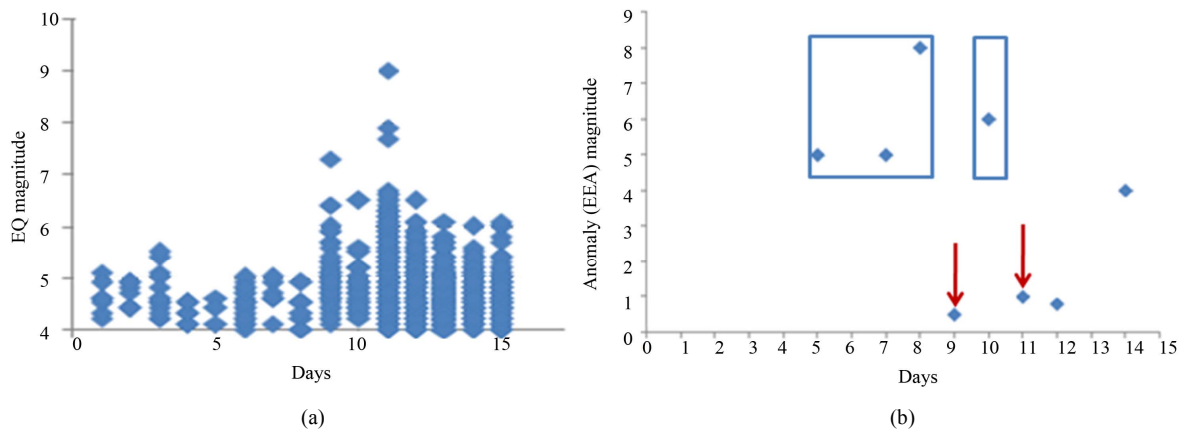


Figure 4. Shows (a) Magnitudes of all EQ events occurring within -10°N to 45°N and 90°E to 145°E during March 1 to 15, 2011 and (b) the Anomaly parameter (an index of EEA strength) during March 1 to 15, 2011. Note in Figure 4 (b), the absence of anomaly from March 1 to 4 and its gradual increase in strength from March 5 to reach a peak on March 8, (shown within the box) prior to March 9, EQ. Also shown in Figure 4 (b) redevelopment of EEA strength on March 10 (enclosed within the box). The decrease of anomaly strength on 9 and 11 are also marked.

developed. Thus, the formation of EEA demonstrates a strong association with high latitude EQs predominantly occurring within the 30°N - 40°N latitudes over the selected longitudes (Figure 6) during this month. The shifting of anomaly status from NEA at 20°E to EEA at 120°E - 140°E (coinciding with epicentre position), prior to these EQs as shown in Figure 7, suggests coupling of the one with the other. The see saw effect of growth of EEA and decay of NEA associated with the impending EQs, is also displayed in Figure 8, when the magnitudes of the two parameters are plotted for the relevant days of March 2011. The presence of strong EEA is seen as a

bright band around the two major EQ days.

Unlike the March 2011 EQs that occurred mostly at high latitudes, April 2012 events were observed in the -5°N to $+5^{\circ}\text{N}$ within our interested longitude zone (90°E to 140°E) as displayed in Figure 9. We select here three significant EQ cases of April 11 (*i.e.* IEQ of $M = 8.6$), April 16 ($M = 6.8$) and April 20 ($M = 6.8$), 2012, to examine association of the EQ with the growth and inhibition of EEA and NEA. The TEC global maps of these three days are presented in Figure 10 to highlight the fact that each contour map demonstrates growth of an EEA instead of the NEA that should have been formed at

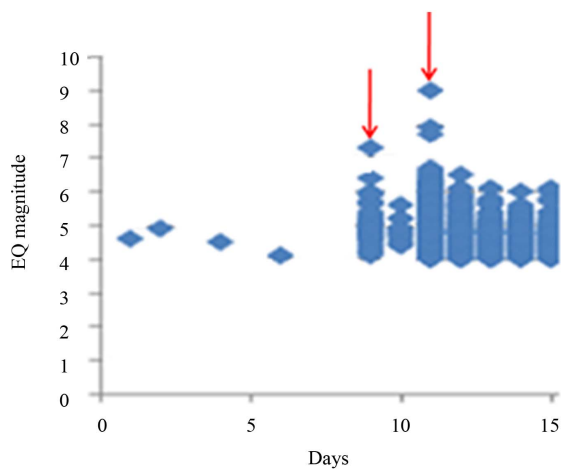


Figure 5. Shows magnitudes of the EQ events occurring only within 30°N to 45°N and 100°E to 140°E during March 1 to 15, 2011. Note from, Figure 4 (b) the increase of anomaly strength on March 8 and 10 (shown within the box) *i.e.*, prior to JEQs of March 9 and March 11, with epicenters at 135°E to 145°E and 35°N to 40°N respectively. The EQ days are shown by arrowheads in Figure 5. Thus, systematic variations in EEA magnitude prior to and during these two EQs are seen with enhancements followed by its decrease on the EQ day (Figure 4(b)).

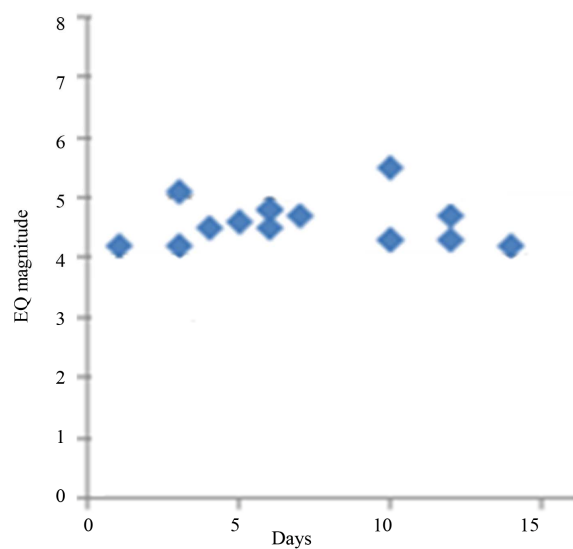


Figure 6. Shows magnitudes of the equatorial EQ events *i.e.*, those occurring within 10°N to -10°N and 90°E to 145°E during March 1 to 15, 2011. Note the absence of association between development of EEA strength (Figure 4(b)) and the equatorial EQ magnitudes (Figure 6).

this hour (10 UT - 11UT) around 20°E - 30°E longitude. It is also significant to note that the EEA positions of 95° E, 140°E and 130°E longitudes coinciding with longitude of the corresponding epicenters which were (a) 2.3°N, 93°E, (b) -5.46°N, 147.12°E and (c) -1.62°N, 134.28°E, respectively.

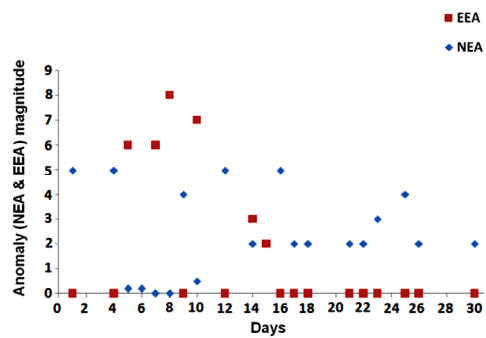


Figure 7. Magnitude of NEA (developed around local noon in 20°E zone) and EEA (developed at night sector in 100°E - 140°E) for the month of March 2011, obtained from global TEC map at 11UT - 12 UT. Note the growth of EEA prior to JEQ and its disappearance after the EQ, the See-Saw relation between appearance of NEA and EEA is also clearly seen.

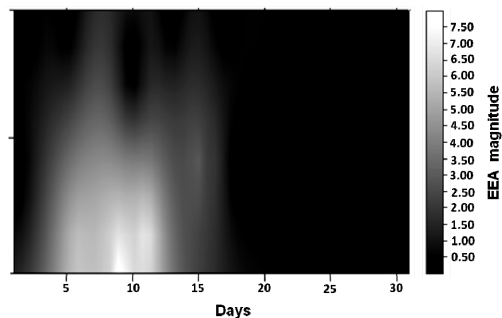


Figure 8. Growth of EEA magnitudes (developed in 100°E - 140°E) obtained from global TEC contour of 11UT - 12 UT, in the month of March 2011. The bright zone corresponds with the major EQ events, indicating growth of strong EEA. EEA magnitudes are shown in shades of gray.

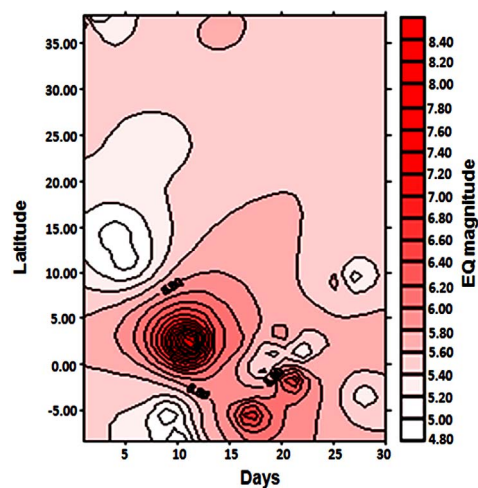


Figure 9. Earthquake events in April 2012 at different latitudes within 80°E to 140°E, longitudes. Note the occurrence of strong events concentrates in the equatorial sector unlike the EQ cases occurred prior JEQ of March 2011. Magnitudes of events are shown in color shades.

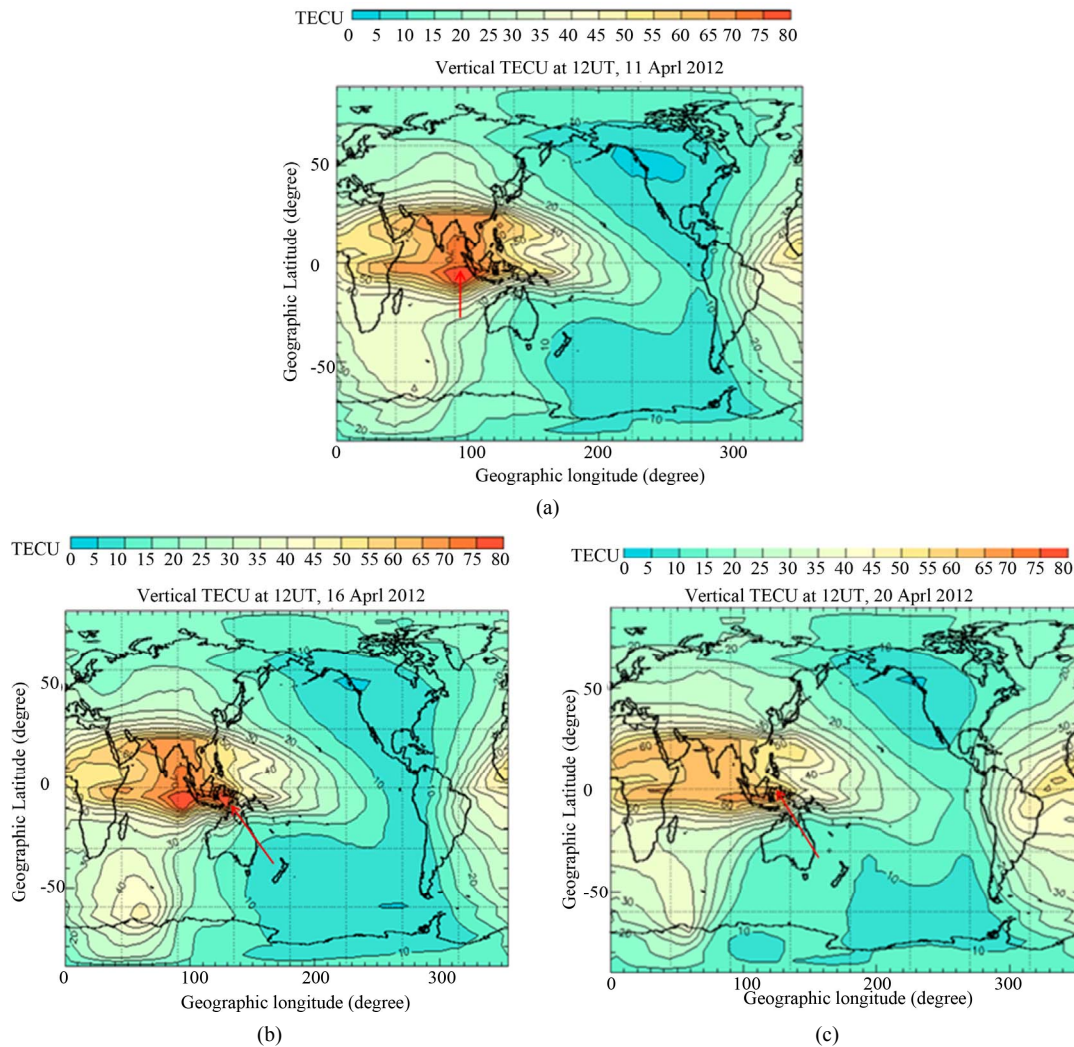


Figure 10. Shows development of EEA at three different longitudinal sectors prior to the three strong EQs occurring with epicenters (a) 2.3°N, 93°E (b) -5.46°N, 147.12°E and (c) -1.62°N, 134.28°E. Positions of the EEAs around the epicentre longitudes are marked by arrow heads.

This analysis along with that for March 2011 events thus supports the fact that the development of EEA is coupled to the strong EQ events whether occurred at the equatorial or at high latitude zone.

3. Discussion and Conclusions

The explanations to the observed development of the EEA and shift of this anomaly zone towards the longitude of epicentre of the two most devastating recent EQs one at mid latitude and the other at the equator, are difficult to put forward with present understandings on equatorial anomaly, though the underlying physics and dynamics involved with the process are well established. The growth of such anomaly is coupled with conductivity of the ionosphere under an impressed electric field that becomes anisotropic in presence of a magnetic field. The

result is generation of three conductivities namely Longitudinal, Pedersen and Hall conductivities. The Hall conductivity amongst the three is significant in this context. Because the Hall current flowing in a direction perpendicular to both the electric and magnetic fields generates a force that moves the plasma upwards through the process $E \times B$ drift that causes transportation of ionization from the equator to regions off the equator, creating a minimum density over the magnetic equator, while causing maxima at latitudes to 20° (geomagnetic) north and south of the equator [8-11]. The effective enhancement of Ionization density or TEC caused by this process at off equatorial stations is generally obtained just after local noon as displayed in **Figure 1**. One can also see formation of such density maximum zones, *i.e.* Normal Equatorial Anomaly (NEA) around local noon (at 20°E longitude) at 12 UT, in the global TEC map of **Figure**

3(a). But the development process of NEA is dissipated prior to the two strong EQs of this study. This apparent inhibition of NEA is replaced by an anomalous development of a high density zone at the near equator in the night sector; a phenomenon we name as EEA. The coincidence of the formation of the EEA with the longitudinal sector of the epicentre, as revealed through analysis of these two major EQs is significant. This observation may not be explained only through the proposals offered by many workers while examining relation between EQ events and modifications in ionization density or in the TEC [6,12,14,19,27,28]. One such hypothesis on EQ time changes in density peak at low-latitudes is due to manifestation of Appleton type $E \times B$ charge movement specially when the epicentre lies near to the equator and in such case E is the EQ induced electric field. It is shown by Devi *et al.* [6,28] that low-latitude earthquakes can also force similar changes to electron density. Devi *et al.* [28], have also observed that when model IRI is used to estimate earthquake time low latitude TEC, the input values on 'F-region peak ionization density', need

to be modified appropriate to "earthquake time variations in TEC", for achieving concordance between model output and TEC observed noontime values. For this purpose changes in F-peak density they considered are the result of dumping of ionisation to low latitude station from the epicentre through Appleton anomaly process, initiated by the EQ generated E-field. These observations and results thus suggest that E-field could contribute significantly in changing ionisation density around epicentre zone. But to correlate association of the EEA *i.e.*, a high density zone near the equator at the night sector with density modification near mid-latitude epicenter is difficult. To examine such relation we map the NmF₂ data available during the period of JEQ, at I-Cheon (37.14°N, 124°E) near epicentre zone and also at Darwin (-12.4°N, 130.9°E) a location where EEA was formed. **Figure 11** shows daily NmF₂ values and their monthly mean (presented by solid and dashed blue lines respectively) over Darwin (a station at the equatorial anomaly zone). The red and black portions of the curves in the **Figure 11** indicate positive and negative ionospheric effects. One can see a large

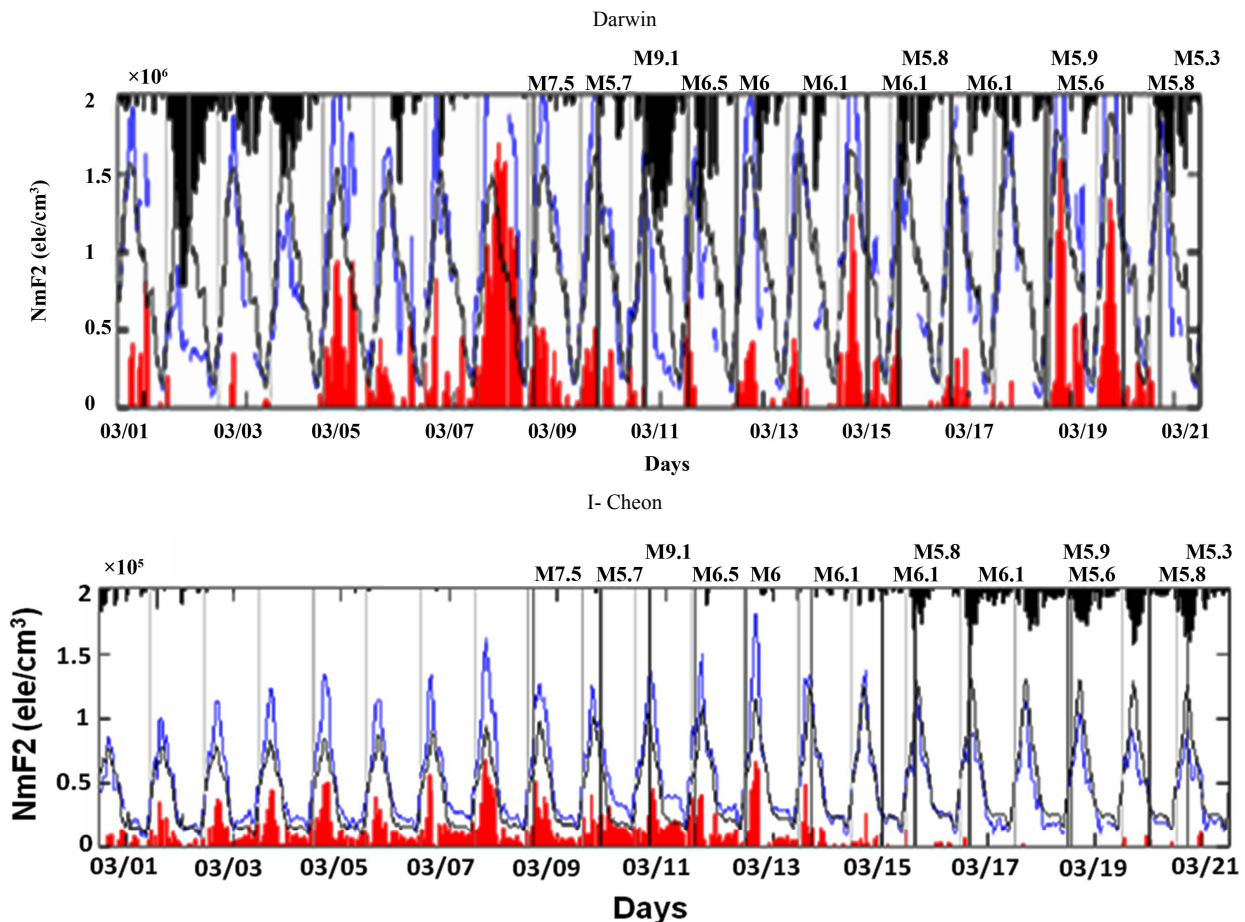


Figure 11. Ionization density enhancement before Japan EQs especially on March 8, 2011, over Darwin (a) and (I-Cheon). Note the anomalous increase in its value (marked by red shade) in Darwin near the EEA zone compared to that observed at I-Chen (near epicenter region).

accumulation of ionisation density especially on the night of March 8, (one day prior to EQ of March 9) at Darwin, and a well developed EEA in global TEC map (**Figure 2 d**) at similar latitude/longitude position. In I-Cheon, the station near to the epicentre, the increase in density is less intense by 50% than that of Darwin, suggesting a possible transportation from epicentre to the EEA zone. One can also note from **Figure 10(a)** the development of strong negative effect on the day of the major JEQ of March 11, especially at Darwin. In this aspect the presence of a magnetic storm as displayed by DST variations of **Figure 11** that coincides with the March 11 EQ is to be noted. This negative density effect can be associated with the magnetic storm, a similar feature is also observed from **Figure 10(a)**, for the storm of March 1 (**Figure 11**). However, the ionospheric storm time dynamics being not the subject of this paper, the negative density variation noted on the major EQ day *i.e.* on March 11 will not be further dealt with.

The IPS TEC global map shown here is produced with IRI model by taking real-time foF2 data obtained from the region. Therefore, the nighttime increase in NmF2 over Darwin supports the growth of EEA as reflected in the TEC global map. But how such anomaly is coupled to the major EQs occurring at latitude as high as of 35°N, is a question. It is equally intriguing to note the adjustment of EEA longitude to epicenter longitudes. Considering all the observed features we can also look for the explanation to the hypotheses of EQ time equatorial/low latitude anomaly that suggest pumping of ionization from epicentre to off epicentre location by the EXB drift but possibly in this case the transportation process is significant during anomaly reversal time. It is well known that the day time anomaly caused by the eastward E field reverses after sunset with the development of westward electric field. Therefore, EXB upward drift decreases during reversal time, goes to negative *i.e.* downward direction and reverse fountain effects become operational [29,30] and westward electric fields may result to nighttime enhancements in electron concentrations in mid latitude F-region [29], coupled with small increase in geomagnetic potential. Along with the mid-latitude increase in density, the downward compression of ionization due to large downward ExB drift can produce the nighttime increase in NmF2/TEC at the equator [31].

The large increase in nighttime TEC near equator prior to the JEQ *i.e.* the EEA, may be the result of such dumping from epicentre due to EQ induced westward E field, suggesting development of coupling processes between high and low latitude during EQ preparatory processes. The horizontal component of magnetic field at the location of the epicentre though weak, but the situation of zero declination contour lines [32,33] that touches epicentre to the near equatorial high density zone of **Figure**

2, supports possible coupling between the mid latitude epicentre and the near equatorial high density location within the same longitude zone. In case of the IEQ, the zero declination contour between epicentre and high density zone of **Figure 3** supports such possibility of transportation to the epicentre longitude. Interestingly the zero-declination contour line follows the tectonic fault line of an active seismic zone, as displayed in **Figure 11**. Further, association of these major EQs with ongoing magnetic pole movement process that is related to inner core and tectonic status needs to be considered in the light of differential rotation of the core. Such rotation generating magnetic field and coupling process between modular structures of earth interior, resulting to a dynamo effect that may generate a two-way traffic of migrating electrons from one strong anomaly zone to another may be in a wide span of longitudes but in the same latitudinal situation, coupled by the similar magnetic declination contour. Such processes may result to dissipation of strong anomaly zone like at 20°E (in this case) and development of anomaly in the night sector.

Along with this explanation, one has to look for other sources which are active prior to an impending EQ, specially in the generation of a dynamical coupling from lower to atmosphere. In such an attempt Molchanov and Hayakawa [34] have shown that seismo-electromagnetic emissions mainly in lower frequencies propagate upwards, locally increasing the temperature of the ionosphere and may penetrate into the ionosphere/magnetosphere, resulting precipitation of magnetospheric high-energy charged particles into the lower ionosphere through wave-particle interactions. But seismogenic wave intensity being weak, such impact will be not effective and cannot be associated with EEA and more so in the background environment of a night sector.

One also looks for lower atmospheric perturbations triggered by seismic generated waves as another source in modulating density of ionosphere. The wavelike structures are generated in EQ environment due to modifications in atmospheric parameters like temperature, pressure, humidity. Because, the increase in temperature by the earthquake preparatory processes could develop a differential temperature situation in the steady nocturnal atmosphere thereby sharpening the density gradient or wind shear. In situations when earth's gravity and the magnitude of stabilizing restoring force introduced by the density gradient are comparable, special structures or waves known as gravity waves are generated. They are quasi longitudinal waves and in presence of strong wind shear these waves break leading to Kelvin Helmholtz instability to generate wave structures. Development of such waves prior to one of the low altitude EQs was also seen by GU Sodar [35], as ramp type structures considered as manifestation of gravity waves [36,37]. Associa-

tion of seismic triggered waves with modification in ionospheric electron density prior to an earthquake was also presented by a number of workers [38-41]. Hegai *et al.*, [40] have computed possible effects of internal gravity waves in nighttime F layer density prior to a strong earthquake, considering origin of the waves with Joule heating due to the seismogenic electric field. They have shown that modification in ionisation density associated with wavelike character depends on the time of arrival of gravity waves at a distance $r = 1000$ km from the epicentre of an impending earthquake. Klomnikoto *et al.*, [41] have presented through model computation the possibility in modulation of electron density by EQ generated gravity waves that could lead to redistribution of electron density from the epicenter zone to equatorial region, a result relevant to our observation. However, to support this mode of transportation of density no such wave signature could be seen in TEC or ionisation density in the data sets of the two case studies we have taken up here.

It is also important to consider the EQ time radon emission from lithosphere near to the epicentre that may trigger ionization in the atmosphere. The seismic fault zone being in severe stressed condition prior to a major EQ, may release radon gas. In ionosphere, the radon gas not only enhances the electron density, but could modulate the atmospheric electric field, leading to ionospheric perturbation [42,43]. In such situation the component of electric current caused by the Lithosphere-Atmosphere-Ionosphere (LAI) coupling as has been suggested by Freund [43] and Sorokin *et al.*, [44] may also be considered, where the group proposed that enhancement of density is due to increase in DC electric field up to 10 mV/m in the ionosphere, thereby generating electric current into the atmosphere-ionosphere circuit. The current they said acts as source of an electromotive force in the ground-air layer through injection of charged aerosols with soil gases in the atmosphere during seismic activity period.

Finally out of all these possible sources we have zeroed down to two main factors in transporting charged particles for development of the EEA zone. One of the factors is the earthquake time downward ExB drift generated by westward electric field that leads to modification in nighttime increase in NmF2/TEC at the equator. Thus, E-H coupling mode in case of the two severe EQ events one in Japan (lies in fault line, as marked in **Figure 12**), and the other in Indonesia (arrow head in **Figure 12**) could enhance TEC strength at locations as shown by the global TEC map. It is interesting to note that TEC values observed at Guwahati, a location touched by the fault line also recorded high density [45], prior to the JEQs. The coupling processes between mid and equatorial regions may thus develop before a strong EQ, the sig-

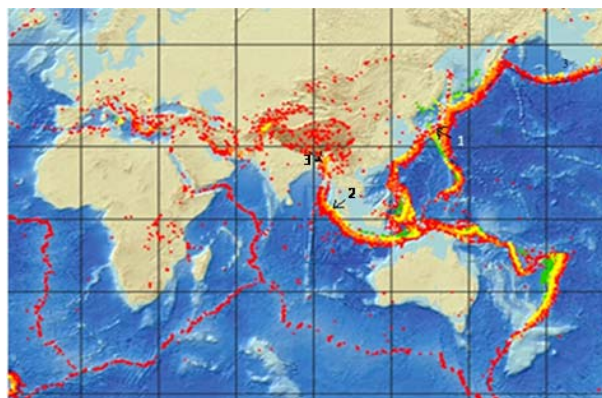


Figure 12. Displays the global seismic fault line. The positions of 1) Japan EQ and 2) Indonesia EQ are shown along with the location of 3) Guwahati, an Equatorial anomaly crest station.

nature of which could be seen as an anomaly at near equatorial region in the epicentre longitude zone. This process of accumulation of ionisation density at the $100^{\circ}\text{E} - 120^{\circ}\text{E}$ longitudes is further enhanced by EM focusing effect generated at the EEA location due to the presence of the distortion of earth magnetic field in this sector. The focusing effect in this case can be explained through the simple theory that if the magnetic field converges towards a small region in an otherwise uniform magnetic field over an area, the flux density within the convergence zone would bring the electron current to a focus. The curve in the earth magnetic field (more so in the near horizontal component) at around 110°E and 15°N , acts like a cone where charged particles if enter magnetic lines, may get trapped and thereby show increase in its density. Before the strong EQ cases as taken up here, the electrons with charge e moving downwards along the magnetic field line by EQ induced electric field (as discussed above) with drift velocity v that experience a force of magnitude $e(v \times B)$, resulting to a Hall force of $H_f = -(v \times B)$. Therefore, with the increase of Hall force, the density increases thereby strengthening the accumulation process of electrons by EQ preparatory processes at the apex of cone zone, in our case at 100°E longitude and 15°N latitude. Increase of drift value *i.e.* of Hall force with magnitude of EQ is the result of spreading of observation of TEC/foF2 far beyond epicentre zone (20, 27, 46, and 47). Here in this paper we consider that this process to be active during the EQ time along with the others and present that the magnetic distortion at special zone may lead to density modulation thereby acting as an identification signature of an EQ event.

As a possible aspect of the future study, we would use the results of this analysis as a basis for constructing quantitative models of the growth and inhibition of equatorial anomaly, to obtain a more reliable and accu-

rate estimations of the EQ in connection with the observable quantities and their relationships.

4. Acknowledgements

The authors acknowledge the data support and suggestions received from the Australian meteorological department. The NmF2 data received from Ko-Ichiro Oyama, Institute of Space Science, National Central University, Taiyuan 32001, Taiwan are duly acknowledged.

REFERENCES

- [1] G. K. Davies and D. M. Baker, "Ionospheric Effects Observed Round the Time of Alaska Earthquake of March 28, 1964," *Journal of Geophysical Research*, Vol. 70, No. 9, 1965, pp. 2251-2263. [doi:10.1029/JZ070i009p02251](https://doi.org/10.1029/JZ070i009p02251)
- [2] E. Calais and J. B. Minster, "GPS Detection of Ionospheric Perturbations Following the January 17, 1994, Northridge Earthquake," *Geophysical Research Letters*, Vol. 22, No. 9, 1995, pp. 1045-1048. [doi:10.1029/95GL00168](https://doi.org/10.1029/95GL00168)
- [3] M. Hayakawa, O. A. Molchanov, T. Ondoh and E. Kawai, "The Precursory Signature Effect of the Kobe Earthquake on VLF Sub Ionospheric Signals," *Journal of Communications Research Laboratory Tokyo*, Vol. 43, 1996, pp. 169-180.
- [4] M. Hayakawa, "Atmospheric and Ionospheric Electromagnetic Phenomena Associated with Earthquakes," Terra Scientific Publishing Co, Tokyo, 1999.
- [5] V. N. Oraevsky, Y. Y. Ruzhin and I. I. Shagimuratov, "Anomalies of Ionospheric TEC above Turkey before Two Strong Earthquakes," *Proceedings of 15th Wroclaw EMC Symposium*, Brugge, 11-15 September 2000, pp. 508-512.
- [6] M. Devi, M. K. Barman A. K. Barbara and A. H. Depueva, "Total Electron Content near Anomaly Crest as Precursor of Earthquake," *India Journal of Radio & Space Physics*, Vol. 30, 2001, pp. 209-213.
- [7] J. Y. Liu, Y. I. Chen, Y. J. Chou and H. F. Tsai, "Variations of Ionospheric Total Electron Content during the Chi-Chi Earthquake," *Geophysical Research Letters*, Vol. 28, No. 7, 2001, pp. 1383-1386. [doi:10.1029/2000GL012511](https://doi.org/10.1029/2000GL012511)
- [8] G. O. Walker and H. F. Chen, "Computer Simulation of the Seasonal Variations of Ionospheric Equatorial Anomaly in East Asia under Solar Minimum Conditions," *Journal of Atmospheric and Terrestrial Physics*, Vol. 51, No. 11-12, 1989, pp. 953-974. [doi:10.1016/0021-9169\(89\)90011-1](https://doi.org/10.1016/0021-9169(89)90011-1)
- [9] G. O. Walker, J. H. K. Ma and E. Golton, "The Equatorial Ionospheric Anomaly in the Electron Content from Solar Minimum to Solar Maximum for the South East Asia," *Annals of Geophysics*, Vol. 12, No. 2-3, 1994, p. 195.
- [10] I. Horvath and E. A. Essex, "Vertical $E \times B$ Drift Velocity Variations and Associated Low-Latitude Ionospheric Irregularities Investigated with the TOPEX and GPS Satellite Data," *Annals of Geophysics, European Geosciences Union*, Vol. 21, 2003, pp. 1017-1030. [doi:10.5194/angeo-21-1017-2003](https://doi.org/10.5194/angeo-21-1017-2003)
- [11] D. Anderson, A. Anghel, J. L. Chau and K. Yumoto, "Global Low-Latitude, Vertical $E \times B$ Drift Velocities Inferred from Daytime Magnetometer Observations," *Space Weather*, Vol. 4, No. 8, 2006. [doi:10.1029/2005SW000193](https://doi.org/10.1029/2005SW000193)
- [12] A. H. Depueva and Yu. Ya. Ruzhin, "Seismoionospheric Fountain Effect as Analogue of Active Space Experiment," *Advances in Space Research*, Vol. 15, No. 12, 1995, pp. 12-15. [doi:10.1016/0273-1177\(95\)00036-E](https://doi.org/10.1016/0273-1177(95)00036-E)
- [13] J. Y. Liu, Y. J. Chino, S. A. Pulintets, H. F. Tsai and X. Zeng, "A Study on the TEC Perturbation Prior to the Reili Chi-Chi and Chi-Yi Earthquake," *Seismo Electromagnetics: Lithosphere-Atmosphere-Ionosphere Coupling, TER RAPUB*, Tokyo, 2002, pp. 293-300.
- [14] M. Devi, A. K. Barbara, A. H. Depueva and V. Depueva, "Preliminary Results of TEC Measurements in Guwahati, India," *Advances in Space Research*, Vol. 42, No. 4, 2008, pp. 753-756. [doi:10.1016/j.asr.2008.01.020](https://doi.org/10.1016/j.asr.2008.01.020)
- [15] N. Fukushima, "Contribution to Geomagnetic Sq Field and Equatorial Electrojet from the Day/Night Asymmetry of Ionospheric Current under dawn-Dusk Electric Fields of Magnetospheric Origin," *Pure and Applied Geophysics PAGEOPH*, Vol. 131, 1989, pp. 437-446. [doi:10.1007/BF00876838](https://doi.org/10.1007/BF00876838)
- [16] Z. I. Min-Yun and C.-S. Shen, "The Equatorial Electrojet and the Magnetosphere-Ionosphere Coupling-I. Analysis of Low-Latitude Geomagnetic Data," *Planetary and Space Science*, Vol. 39, No. 6, 1991, pp. 907-917. [doi:10.1016/0032-0633\(91\)90095-R](https://doi.org/10.1016/0032-0633(91)90095-R)
- [17] K. C. Yeh, S. J. Franke, E. S. Andreeva and V. E. Kunitstyn, "An Investigation of Motions of the Equatorial Anomaly Crest," *Geophysical Research Letters*, Vol. 28, No. 24, 2001, pp. 4517-4520. [doi:10.1029/2001GL013897](https://doi.org/10.1029/2001GL013897)
- [18] M. Devi, M. K. Barman and A. K. Barbara, "Identification of Quiet and Disturbed Days through TEC Profile Features over Anomaly Crest Station," *Journal of Atmospheric and Solar Terrestrial Physics*, Vol. 64, No. 12-14, 2002, pp. 1413-1423. [doi:10.1016/S1364-6826\(02\)00105-0](https://doi.org/10.1016/S1364-6826(02)00105-0)
- [19] M. Devi, A. K. Barbara and A. H. Depueva, "Association of Total Electron Content and foF2 Variations with Earthquake Events at the Anomaly Crest Region," *Annals of Geophysics*, Vol. 47, No. 1, 2004, pp. 83-91.
- [20] A. Depueva, A. Mikhailov, M. Devi and A. K. Barbara, "Spatial and Time Variations in Critical Frequencies of the Ionospheric F Region above the Zone of Equatorial Earthquake Preparation," *Geomagnetism and Aeronomy*, Vol. 47, 2007, pp. 129-133. [doi:10.1134/S0016793207010197](https://doi.org/10.1134/S0016793207010197)
- [21] M. Devi, A. J. D. Sarma, S. Kalita, A. K. Barbara and A. Depueva, "Adoptive Techniques on Extraction of Pre-Seismic Parameters on Total Electron Content (TEC) at Anomaly Crest Stations Using GPS Data," *Geomatics, Natural Hazards and Risk*, Vol. 3, No. 3, 2011, pp. 193-

206. [doi:10.1080/19475705.2011.595831](https://doi.org/10.1080/19475705.2011.595831)
- [22] M. Devi and A. K. Barbara, "On beyond the Horizon Propagation of VHF Signals," ISEA-7, Hong Kong, 1984, pp. 6-26.
- [23] M. Hayakawa and O. A. Molchanov, "Seismo Electromagnetics, Lithosphere-Atmosphere-Ionosphere Coupling," Terra Scientific Publishing Co, Tokyo, 2002.
- [24] M. Devi, A. K. Barbara, Yu. Ya. Ruzhin and A. H. Depueva, "Beyond the Horizon Propagation of VHF Signals, Atmospheric Features and Earthquake," *Electronic Journal, Investigated in Russia*, Vol. 39, 2007, pp. 1331-1340.
- [25] M. Devi, A. K. Barbara, A. H. Depueva, Yu. Ya. Ruzhin, and V. Depueva, "Anomalous Total Electron Content (TEC) and Atmospheric Refractivity Prior to Very Strong China Earthquake of May 2008," *International Journal of Remote Sensing*, Vol. 31, No. 13, 2010, pp. 3589-3599. [doi:10.1080/01431161003727663](https://doi.org/10.1080/01431161003727663)
- [26] M. Devi, A. K. Barbara, Ya. Yu. Ruzhin and M. Hayakawa, "Over-the-Horizon Anomalous VHF Propagation and Earthquake Precursors," *Surveys in Geophysics, Springer Publication*, Vol. 33, No. 5, 2012, pp. 1081-1106. [doi:10.1007/s10712-012-9185-z](https://doi.org/10.1007/s10712-012-9185-z)
- [27] A. H. Depueva and N. M. Rotanova, "Low-Latitude Ionospheric Disturbances Associated with Earthquakes," *Annals of Geophysics*, Vol. 44, No. 2, 2001, pp. 221-228.
- [28] M. Devi, A. K. Barbara, P. Kashyap, A. Depueva, Ya. Yu. Ruzhin and V. Depueva, "Earthquake Time Low Latitude TEC and Model Estimated Values: Identification on Earthquake Induced Atmospheric Dynamics," *Advances of Geosciences*, Vol. 26, 2010, pp. 69-84.
- [29] C. G. Park, "Westward Electric Fields as the Cause of Nighttime Enhancements in Electron Concentrations in Mid Latitude F-Region," *Journal of Geophysical Research*, Vol. 76, No. 19, 1971, pp. 4560-4568. [doi:10.1029/JA076i019p04560](https://doi.org/10.1029/JA076i019p04560)
- [30] N. Balan and G. J. Bailey, "Equatorial Plasma Fountain and Its Effects: Possibility of an Additional Layer," *Journal of Geophysical Research*, Vol. 100, No. A11, 1995, pp. 21421- 21432.
- [31] B. C. N. Rao, "The Post Sunset Rise in foF2 in the Transition Region and Its Dependence on the Post Sunset Rise in h'F in the Equatorial Region," *Journal of Geophysical Research*, Vol. 68, No. 9, 1963, pp. 2551-2557. [doi:10.1029/JZ068i009p02551](https://doi.org/10.1029/JZ068i009p02551)
- [32] R. P. Kane, "Geomagnetic Field Variations," *Space Science Reviews*, Vol. 18, No. 4, 1976, p. 413.
- [33] S. Mavlean, S. Macmillan, S. Mavs, V. Lesur, A. Thomson and D. Dater, "US-UK World Magnetic Model for 2005-2019," NOAA, Technical Report NESDIS/NGDC-1, 2004, p. 54.
- [34] O. A. Molchanov and M. Hayakawa, "Seismo-Electromagnetics and Related Phenomena: History and Latest Results," TERRAPUB, Tokyo, 2008.
- [35] M. Devi, A. K. Barbara and M. K. Barman, "Heat Exchange between Adiabatically Transported Air Parcels and the ABL," *Indian Journal of Physics*, Vol. 743, No. 3, 2000, pp. 345-347.
- [36] J. Naithani and H. N. Dutta, "Atmospherric Boundary Layer Studies over the Indian Antarctic Station Maitri," Report, Radio Science Division, National Physical Laboratory, New Delhi.
- [37] Report of Kyoto University Radio Science Centre for Space and Atmosphere, 2001, p. 19.
- [38] O. A. Molchanov, M. Hayakawa and K. Miyaki, "VLF/LF Sounding of the Lower Ionosphere to Study the Role of Atmospheric Oscillations in the Lithosphere-Ionosphere Coupling," *Advances in Polar Upper Atmosphere Research*, No. 15, 2001, pp. 146-158.
- [39] A. V. Shvets, M. Hayakawa and O. A. Molchanov, "Subionospheric VLF Monitoring for Earthquake Related Ionospheric Perturbations," *Journal of Atmospheric Electricity*, Vol. 22, 2002, pp. 87-99.
- [40] V. V. Hegai, V. P. Kima and J. Y. Liu, "The Ionospheric Effect of Atmospheric Gravity Waves Excited Prior to Strong Earthquake," *Advances in Space Research*, Vol. 37, No. 4, 2006, pp. 653-659. [doi:10.1016/j.asr.2004.12.049](https://doi.org/10.1016/j.asr.2004.12.049)
- [41] M. V. Klimenko, V. V. Klimenko, I. V. Korpov and I. E. Zakharenkova, "Simulation of Seismo-Ionospheric Effects Initiated by Internal Gravity Waves," *Russian Journal of Physical Chemistry*, Vol. 5, No. 3, 2011, pp. 393-401. [doi:10.1134/S1990793111030109](https://doi.org/10.1134/S1990793111030109)
- [42] S. Pulinets, "Lithosphere-Atmosphere-Ionosphere Coupling (LAIC) Model," In: M. Hayakawa, Ed., *Electromagnetic Phenomena Associated with Earthquakes*, Transworld Research Network, Trivandrum, 2009, pp. 235-253.
- [43] F. Freund, "Stress-Activated Positive Hole Charge Carriers in Rocks and the Generation of Pre-Earthquake Signals," In: M. Hayakawa, Ed., *Electromagnetic Phenomena Associated with Earthquakes*, Transworld Research Network, Trivandrum, 2009, pp. 41-96.
- [44] V. M. Sorokin, Y. Y. Ruzhin, A. K. Yaschenko and M. Hayakawa, "Generation of VHF Radio Emissions by Electric Discharges in the Lower Atmosphere over a Seismic Region," *Journal of Atmospheric and Solar-Terrestrial Physics*, Vol. 73, No. 5-6, 2011, pp. 664-670. [doi:10.1016/j.jastp.2011.01.016](https://doi.org/10.1016/j.jastp.2011.01.016)
- [45] M. Devi and A. K. Barbara, "Total Electron Content and Anomalous Appearance of GPS Satellites as Pointers to Epicentre Identification of Major Japan Earthquake of 2011," *Positioning*, Vol. 3, No. 1, 2012, pp. 7-12. <http://www.SciRP.org/journal/pos>
- [46] J. Y. Liu, Y. I. Chen, C. H. Chen and K. Hattori, "Temporal and Spatial Precursors in the Ionospheric Global Positioning System (GPS) Total Electron Content Observed before the 26 December 2004 M9.3 Sumatra—Andaman Earthquake," *Journal of Geophysical Research*, Vol. 115, No. A9, 2010. [doi:10.1029/2010JA015313](https://doi.org/10.1029/2010JA015313)
- [47] B. Zhao, T. Yu, M. Wang, W. Wan, J. Lei, L. Liu and B. Ning, "Is an Unusual Large Enhancement of Ionospheric Electron Density Linked with the 2008 Great Wenchuan Earthquake?," *Journal of Geophysical Research*, Vol. 113, No. A11, 2008. [doi:10.1029/2008JA013613](https://doi.org/10.1029/2008JA013613)